Anticancer effects of theaflavin-1 in gastric cancer cells via ROS-mediated p53 activation

Yi-Xin Liu[1,3,4], Zhuan Wang[1,2], Chang-Rong Tian[1,2], Shu-Han Wang[1], Ying Rao[1], Yong-Le Li[1], Rong He[1], Ming-Tao Luo[1], Li-He Jiang[1,2,3,4]*

1. School of Basic Medical Sciences, Youjiang Medical University for Nationalities, Baise, 533000, Guangxi, P.R. China

2. College of Light Industry and Food Engineering, Medical College, Guangxi University, Nanning, 530004, Guangxi, P.R. China

3. Hubei Key Laboratory of Food Nutrition and Safety (Huazhong University of Science and Technology), Wuhan, 430030, Hubei, P.R. China

4. Shaanxi Tea Key Lab Co-sponsored by Province and Municipality, Ankan, 725000, Shaanxi, P.R. China

Yi-Xin Liu: https://orcid.org/0009-0003-1090-5604

Corresponding author:

Li-He Jiang

School of Basic Medical Sciences, Youjiang Medical University for Nationalities, Baise, 533000, Guangxi, China.

Tel.: +86 776 2849482; fax: +86 776 2849482, Mobile phone: +86 18577190501

E-mail address: jianglihe@ymun.edu.cn (L.H. JANG);jianglihe@gxu.edu.cn.

ORCID number: 0000-0002-9043-3162

Submitted: 2025/9/17

Revised: 2026/2/17

Accepted: 2026/3/22

Abstract

Background: Theaflavin-1 (TF1), a major polyphenolic component of black tea, has shown anticancer activity in several tumor models. However, its effects and molecular mechanisms in gastric cancer remain insufficiently characterized.

Methods: For this purpose,Cell viability was evaluated in SGC-7901, MGC-803, and GES-1 cells using CCK-8 and colony formation assays. Hoechst 33258 staining was used to observe apoptotic nuclear morphology, flow cytometry was used to quantify apoptosis, and the wound-healing assay was used to assess cell migration. Transcriptome sequencing, qRT-PCR, mitochondrial membrane potential analysis, reactive oxygen species (ROS) detection, and western blotting were performed to investigate the underlying mechanisms.

Results: TF1 significantly inhibited the viability, clonogenicity, and migration of SGC-7901 and MGC-803 cells in a dose-dependent manner, while exerting minimal toxicity toward normal GES-1 cells. TF1 also induced apoptosis and mitochondrial membrane depolarization. Transcriptome sequencing identified the p53 signaling pathway as a major pathway altered by TF1 treatment. Western blotting showed that TF1 increased the expression of Bax, p53, p21, cytochrome c, and cleaved caspase-3, whereas it decreased the expression of Bcl-2, CDK6, PCNA, N-cadherin, and Vimentin. TF1 also elevated intracellular ROS levels, and pretreatment with N-acetylcysteine partially reversed these changes.

Conclusion: TF1 suppresses gastric cancer cell growth and migration and promotes apoptosis through a ROS-p53-mitochondrial signaling axis. These findings support TF1 as a promising natural candidate for further investigation in gastric cancer therapy.

Keywords: gastric cancer; theaflavin-1; ROS; p53; mitochondrial apoptosis

Introduction

Gastric cancer remains one of the most common malignant tumors worldwide and is still associated with substantial mortality despite advances in diagnosis and treatment.[1] Current therapeutic strategies, including surgery, chemotherapy, radiotherapy, and chemoradiotherapy, have improved outcomes in some patients, but recurrence, late diagnosis, adverse effects, and drug resistance continue to limit long-term benefit.[2,3] Therefore, the identification of more effective and less toxic therapeutic agents is still needed.

Natural products are an important source of biologically active compounds with anticancer potential.[4] Black tea contains abundant polyphenols, including catechins and theaflavins, and tea-derived bioactive compounds have shown broad pharmacological and antitumor activities.[5] Theaflavin-1 (TF1), a benzotropolone-containing polyphenol formed during black tea fermentation, is a representative theaflavin.[6] Previous studies have shown that theaflavins can inhibit proliferation, induce apoptosis, and suppress migration in several cancer types, including colon, ovarian, prostate, and hepatocellular carcinomas.[7–11]

Although the anticancer effects of theaflavins have been reported in other tumor models, the activity of TF1 in gastric cancer and its molecular basis remain incompletely understood. Previous studies in gastric cancer have highlighted the importance of p53-related signaling, while broader evidence indicates that p53 and ROS are central regulators of tumor cell stress responses and apoptosis.[12–15] Based on our preliminary transcriptomic data and previous reports implicating ROS and p53 in cancer cell death, we that TF1 may inhibit gastric cancer progression through activation of a ROS-p53-mitochondrial apoptosis axis.

Accordingly, this study investigated the effects of TF1 on the proliferation, migration, and apoptosis of gastric cancer cells in vitro and explored the associated

molecular mechanisms. Our findings provide a theoretical basis for the further development of TF1 as a candidate compound for gastric cancer prevention and treatment.

Materials and methods

Chemicals and reagents

TF1 (purity >= 98%) was purchased from Chengdu Biopurify Phytochemicals Ltd. (Chengdu, China). A 200 mM stock solution was prepared in DMSO and stored at -20 C in aliquots. Cisplatin was purchased from Jiangsu Hausen Pharmaceutical Group Co., Ltd. (Jiangsu, China). N-acetyl-L-cysteine (NAC) was purchased from Sigma-Aldrich (St. Louis, MO, USA). TRIzol reagent, PrimeScript RT kit, and other molecular reagents were obtained from the manufacturers indicated in the original manuscript. Primary antibodies against E-cadherin, N-cadherin, Vimentin, Bax, Bcl-2, caspase-3, PCNA, CDK6, p53, p21, cytochrome c, and beta-actin were purchased from commercial suppliers as listed in the original manuscript.

Cell culture

Human gastric cancer SGC-7901 and MGC-803 cells and normal gastric epithelial GES-1 cells were cultured in RPMI-1640 medium supplemented with 10% fetal bovine serum at 37 C in a humidified incubator containing 5% CO2.

CCK-8 assay

SGC-7901, MGC-803, and GES-1 cells were seeded in 96-well plates and treated with different concentrations of TF1 for 24, 48, or 72 h. Cisplatin was used as a positive control. Cell viability was determined using the CCK-8 assay, and absorbance was measured at 450 nm.

Colony formation assay

SGC-7901 and MGC-803 cells were seeded in 6-well plates at 800 cells/well and treated with TF1 (0, 25, 50, 100, or 200 uM). After 14 days, colonies were fixed with

4% paraformaldehyde, stained with 0.1% crystal violet, photographed, and counted

Wound healing assay (scratch test)

Confluent monolayers of SGC-7901 and MGC-803 cells were scratched with a pipette tip and then treated with TF1. Images were obtained at 0 and 24 h, and the migration rate was quantified using ImageJ.

Hoechst 33258 staining and flow cytometry

Cells were treated with TF1 for 24 h. Hoechst 33258 staining was used to observe apoptotic nuclear morphology. Annexin V/PI staining followed by flow cytometry was used to quantify apoptosis.

RNA transcriptome sequencing and qRT-PCR

Total RNA was extracted from MGC-803 cells treated with 100 uM TF1 for 24 h and subjected to transcriptome sequencing using the Illumina NovaSeq platform. Differentially expressed genes were analyzed using DESeq with thresholds of $|\log2FC| > 1$ and adjusted $P < 0.05$. Selected genes were validated by qRT-PCR, and relative expression levels were calculated using the 2^-Delta Delta Ct method.[16,17]

Mitochondrial membrane potential and ROS analysis

JC-1 staining was used to assess mitochondrial membrane potential. Intracellular ROS levels were measured using DCFH-DA staining. ROS-related experiments were interpreted with reference to current recommendations for oxidative stress measurements.[18]

Western blotting analysis

Total protein was extracted from treated cells, separated by SDS-PAGE, transferred to PVDF membranes, and probed with specific primary and secondary antibodies. Protein bands were visualized using enhanced chemiluminescence.

Statistical analysis

Statistical analyses were performed using GraphPad Prism 8.0.2 software. Data

are presented as mean +- SD from three independent experiments. Student's t-test was used for comparisons between two groups, and one-way ANOVA was used for comparisons among multiple groups. A P value < 0.05 was considered statistically significant.

Results

TF1 inhibited gastric cancer cell viability with limited toxicity toward normal cells

The CCK-8 assays showed that TF1 reduced the viability of SGC-7901 and MGC-803 cells in a dose- and time-dependent manner (Figure 2A, 2B), whereas its effect on GES-1 cells was minimal (Figure 2C). The corresponding IC50 values are shown in Tables 2 and 3.

TF1 suppressed clonogenic growth and migration

Colony formation assays demonstrated that TF1 significantly reduced the clonogenic potential of both gastric cancer cell lines (Figure 3). In wound-healing assays, TF1 markedly inhibited cell migration. Consistently, western blotting showed increased E-cadherin expression and decreased N-cadherin and Vimentin expression after TF1 treatment (Figure 4), suggesting inhibition of epithelial-mesenchymal transition.

TF1 induced apoptosis in gastric cancer cells

Hoechst 33258 staining revealed chromatin condensation and nuclear fragmentation in TF1-treated cells (Figure 5A, 5C). Flow cytometry confirmed a dose-dependent increase in apoptotic cells in both SGC-7901 and MGC-803 cell lines (Figure 5B, 5D).

Transcriptome sequencing implicated the p53 pathway

RNA-seq analysis identified 224 upregulated and 162 downregulated genes after TF1 treatment (Figure 6A). Gene Ontology and KEGG analyses indicated significant enrichment of genes involved in the p53 signaling pathway (Figure 6B). qRT-PCR

validation of selected genes was consistent with the transcriptomic results (Figure 6C, D).

TF1 activated p53-related and mitochondrial apoptotic signaling

Western blotting showed that TF1 increased the protein levels of Bax, cleaved caspase-3, p53, p21, and cytochrome c, while reducing the levels of Bcl-2, CDK6, and PCNA. These results indicate activation of p53 signaling, cell-cycle inhibition, and mitochondrial apoptosis (Figure 7).

TF1 increased ROS accumulation and mitochondrial dysfunction

TF1 caused a dose-dependent loss of mitochondrial membrane potential (Figure 8A) and a marked increase in intracellular ROS levels (Figure 8B). Pretreatment with NAC attenuated TF1-induced changes in apoptosis-related proteins (Figure 8C,D), indicating that ROS generation is an upstream event in TF1-mediated mitochondrial apoptosis.

Discussion

In the present study, TF1 markedly inhibited the proliferation, colony formation, and migration of SGC-7901 and MGC-803 cells, while showing much lower toxicity toward normal GES-1 cells. These findings are consistent with previous reports indicating that theaflavins exert anti-cancer activities in multiple tumor types and may selectively suppress malignant cell growth.[11] TF1 also significantly reduced the migratory ability of gastric cancer cells and modulated epithelial-mesenchymal transition-related markers by decreasing N-cadherin and Vimentin expression and increasing E-cadherin expression. Since dysregulation of these proteins is closely associated with EMT progression and metastatic potential[19–21], our data suggest that TF1 may inhibit gastric cancer cell migration, at least in part, through suppression of EMT.

To explore the molecular basis of these biological effects, we performed transcriptome sequencing and found that the p53 signaling pathway was one of the most significantly enriched pathways after TF1 treatment. This result was further supported by western blot analysis, which showed increased expression of p53 and its downstream effector p21, together with decreased expression of proliferation-related proteins such as CDK6 and PCNA. These findings suggest that TF1 suppresses gastric cancer cell growth through activation of p53-associated cell-cycle arrest and apoptotic signaling. In addition, previous studies have shown that p53 signaling is closely linked to invasion- and EMT-related regulatory networks, supporting the possibility that TF1-induced p53 activation may contribute not only to apoptosis but also to reduced motility.[22,23]

ROS appears to be an important upstream event in this process. In our study, TF1 treatment markedly increased intracellular ROS levels and reduced mitochondrial membrane potential in both gastric cancer cell lines. Pretreatment with NAC partially

reversed the TF1-induced changes in apoptosis-related proteins, indicating that oxidative stress contributes to the pro-apoptotic effect of TF1. Excessive ROS is known to disrupt redox homeostasis, damage mitochondrial function, and activate stress-responsive death pathways in cancer cells.[24] Therefore, our findings support a model in which TF1 elevates ROS, thereby promoting p53 activation and mitochondrial dysfunction.

Mitochondrial apoptosis is characterized by loss of mitochondrial membrane integrity, cytochrome c release, and subsequent caspase activation.[25,26] In agreement with this mechanism, TF1 treatment decreased mitochondrial membrane potential, increased the expression of Bax, cytochrome c, and cleaved caspase-3, and reduced Bcl-2 expression. Since the Bax/Bcl-2 balance is a critical determinant of mitochondrial outer membrane permeabilization, these results indicate that TF1 induces apoptosis through the intrinsic mitochondrial pathway.[27–29] Taken together, our data support the conclusion that TF1 suppresses gastric cancer cell survival and migration through a ROS-mediated p53-mitochondrial apoptotic axis.

This study has several limitations. First, all experiments were conducted in vitro, and in vivo validation is still required. Second, although our data support the involvement of ROS and p53 signaling, the direct upstream molecular target of TF1 remains unclear. Further studies using animal models and more detailed mechanistic approaches will be necessary to confirm the anti-gastric cancer potential of TF1 and to determine whether it may be developed as a therapeutic or adjuvant agent.

Conclusions

In summary, TF1 suppresses the proliferation and migration of human gastric cancer cells and induces apoptosis through a ROS-mediated p53-mitochondrial signaling pathway. TF1 also exhibits relatively low cytotoxicity toward normal gastric epithelial cells, indicating its potential selectivity against malignant cells. These

findings suggest that TF1 may serve as a promising natural compound for the prevention and treatment of gastric cancer. However, further in vivo and preclinical studies are needed to validate its efficacy and safety.

Author Contributions

Yi-Xin Liu: Investigation, Data curation, Formal analysis, Writing - original draft.

Zhuan Wang: Investigation, Data curation, Formal analysis, Writing - original draft.

Chang-Rong Tian: Investigation, Data curation, Writing - review & editing.

Shu-Han Wang: Investigation, Data curation, Writing - review & editing.

Ying Rao: Investigation, Data curation, Writing - review & editing.

Yong-Le Li: Investigation, Data curation, Writing - review & editing.

Rong He: Investigation, Data curation, Writing - review & editing.

Ming-Tao Luo: Investigation, Data curation, Writing - review & editing.

Li-He Jiang: Conceptualization, Supervision, Funding acquisition, Project administration, review & editing.

Funding

This research was supported by the Grant of Guangxi Natural Science Foundation (Grant No.2025GXNSFHA069094, 2025JJA140748), the Baise City Science and Technology Plan Project(Science and Technology Infrastructure Support Program)(Grant No.2025ZJ0707), the Hubei Key Laboratory of Food Nutrition and Safety at Huazhong University of Science and Technology (Grant No.FNS-HBKL2023A02), the Open Research Project of Shaanxi Tea Key Laboratory Co-sponsored by Province and Municipality (Grant No.SXKTL202202), Fujian Provincial Key Laboratory of Innovative Drug Target Research (Grant No. FJ-YW-2025KF06); The National-level Project of University Students' Innovation and Entrepreneurship in 2023 (Grant No. 202310599009).

Declaration of Interest

The authors declare that they have no known competing financial interests or personal relationships that could have appeared to influence the work reported in this paper.

Referance

1. Sung H, Ferlay J, Siegel RL, Laversanne M, Soerjomataram I, Jemal A, et al. Global Cancer Statistics 2020: GLOBOCAN Estimates of Incidence and Mortality Worldwide for 36 Cancers in 185 Countries. CA Cancer J Clin 2021;71(3):209–249; doi: 10.3322/caac.21660.

2. Waddingham W, Nieuwenburg SAV, Carlson S, Rodriguez-Justo M, Spaander M, Kuipers EJ, et al. Recent advances in the detection and management of early gastric cancer and its precursors. Frontline Gastroenterol 2021;12(4):322–331; doi: 10.1136/flgastro-2018-101089.

3. Seeneevassen L, Bessède E, Mégraud F, Lehours P, Dubus P, Varon C. Gastric Cancer: Advances in Carcinogenesis Research and New Therapeutic Strategies. Int J Mol Sci 2021;22(7):3418; doi: 10.3390/ijms22073418.

4. Marwan Almosnid N, Zhou X, Jiang L, Ridings A, Knott D, Wang S, et al. Evaluation of extracts prepared from 16 plants used in Yao ethnomedicine as potential anticancer agents. J Ethnopharmacol 2018;211:224–234; doi: 10.1016/j.jep.2017.09.032.

5. Luo Q, Luo L, Zhao J, Wang Y, Luo H. Biological potential and mechanisms of Tea's bioactive compounds: An Updated review. J Adv Res 2024;65:345–363; doi: 10.1016/j.jare.2023.12.004.

6. Zhang G, Pan Y, Cheng H, Gong S, Chu Q, Chen P. Theaflavin: a natural candidate to restrain thrombosis. Food Funct 2022;13(14):7572–7581; doi: 10.1039/d2fo00152g.

7. O'Neill EJ, Termini D, Albano A, Tsiani E. Anti-Cancer Properties of Theaflavins. Molecules 2021;26(4):987; doi: 10.3390/molecules26040987.

8. Tan Q, Peng L, Huang Y, Huang W, Bai W, Shi L, et al. Structure-Activity Relationship Analysis on Antioxidant and Anticancer Actions of Theaflavins on Human Colon Cancer Cells. J Agric Food Chem 2019;67(1):159–170; doi: 10.1021/acs.jafc.8b05369.

9. Gao Y, Yin J, Tu Y, Chen YC. Theaflavin-3,3'-Digallate Suppresses Human Ovarian Carcinoma OVCAR-3 Cells by Regulating the Checkpoint Kinase 2 and p27 kip1 Pathways. Molecules 2019;24(4):673; doi: 10.3390/molecules24040673.

10. Sun L, Wen S, Li Q, Lai X, Chen R, Zhang Z, et al. Theaflavin-3,3'-di-gallate represses prostate cancer by activating the PKCδ/aSMase signaling pathway through a 67 kDa laminin receptor. Food Funct 2022;13(8):4421–4431; doi: 10.1039/d1fo04198c.

11. Shao J, Meng Q, Li Y. Theaflavins suppress tumor growth and metastasis via the blockage of the STAT3 pathway in hepatocellular carcinoma. Onco Targets Ther 2016;9:4265–4275; doi: 10.2147/OTT.S102858.

12. Li X-F, Xu B-Z, Wang S-Z. Aspirin inhibits the proliferation and migration of gastric cancer cells in p53-knockout mice. Oncol Lett 2016;12(5):3183–3186; doi: 10.3892/ol.2016.5067.

13. Q H, W L, Y Y, S C, J L, J Y, et al. Huashi Jiedu Decoction Enhances 5-Fluorouracil Efficacy in Gastric Cancer via miRNA-21-3p/p53 Pathway. Drug design, development and therapy 2025;19; doi: 10.2147/DDDT.S513371.

14. Vousden KH, Lane DP. p53 in health and disease. Nat Rev Mol Cell Biol 2007;8(4):275–283; doi: 10.1038/nrm2147.

15. Nakamura H, Takada K. Reactive oxygen species in cancer: Current findings and future directions. Cancer Sci 2021;112(10):3945–3952; doi: 10.1111/cas.15068.

16. Livak KJ, Schmittgen TD. Analysis of relative gene expression data using real-time quantitative PCR and the 2(-Delta Delta C(T)) Method. Methods 2001;25(4):402–408; doi: 10.1006/meth.2001.1262.

17. Maren NA, Duduit JR, Huang D, Zhao F, Ranney TG, Liu W. Stepwise Optimization of Real-Time RT-PCR Analysis. Methods Mol Biol 2023;2653:317–332; doi: 10.1007/978-1-0716-3131-7_20.

18. Murphy MP, Bayir H, Belousov V, Chang CJ, Davies KJA, Davies MJ, et al. Guidelines for measuring reactive oxygen species and oxidative damage in cells and in vivo. Nat Metab 2022;4(6):651–662; doi: 10.1038/s42255-022-00591-z.

19. Satelli A, Li S. Vimentin in cancer and its potential as a molecular target for cancer therapy. Cell Mol Life Sci 2011;68(18):3033–3046; doi: 10.1007/s00018-011-0735-1.

20. Yang J, Weinberg RA. Epithelial-mesenchymal transition: at the crossroads of development and tumor metastasis. Dev Cell 2008;14(6):818–829; doi: 10.1016/j.devcel.2008.05.009.

21. Wang P, Zhu Z. Prognostic and Clinicopathological Significance of E-Cadherin in Pancreatic Cancer Patients: A Meta-Analysis. Front Oncol 2021;11:627116; doi: 10.3389/fonc.2021.627116.

22. Alam F, Mezhal F, El Hasasna H, Nair VA, Aravind SR, Saber Ayad M, et al. The role of p53-microRNA 200-Moesin axis in invasion and drug resistance of breast cancer cells. Tumour Biol 2017;39(9):1010428317714634; doi: 10.1177/1010428317714634.

23. Kaller M, Hermeking H. Interplay Between Transcription Factors and MicroRNAs Regulating Epithelial-Mesenchymal Transitions in Colorectal Cancer. Adv Exp Med Biol 2016;937:71–92; doi: 10.1007/978-3-319-42059-2_4.

24. Pei X-D, Yao H-L, Shen L-Q, Yang Y, Lu L, Xiao J-S, et al. α-Cyperone inhibits the proliferation of human cervical cancer HeLa cells via ROS-mediated PI3K/Akt/mTOR signaling pathway. Eur J Pharmacol 2020;883:173355; doi: 10.1016/j.ejphar.2020.173355.

25. Li Q-X, Yu DH, Liu G, Ke N, McKelvy J, Wong-Staal F. Selective anticancer strategies via intervention of the death pathways relevant to cell transformation. Cell Death Differ 2008;15(8):1197–1210; doi: 10.1038/cdd.2008.48.

26. Nadalutti CA, Ayala-Peña S, Santos JH. Mitochondrial DNA damage as driver of cellular outcomes. Am J Physiol Cell Physiol 2022;322(2):C136–C150; doi: 10.1152/ajpcell.00389.2021.

27. Wu C, Luo H, Ma W, Ren X, Lu C, Li N, et al. Polysaccharides isolated from Hedyotis diffusa inhibits the aggressive phenotypes of laryngeal squamous carcinoma cells via inhibition of Bcl-2, MMP-2, and μPA. Gene 2017;637:124–129; doi: 10.1016/j.gene.2017.09.041.

28. Luo Y, Fu X, Ru R, Han B, Zhang F, Yuan L, et al. CpG Oligodeoxynucleotides Induces Apoptosis of Human Bladder Cancer Cells via Caspase-3-Bax/Bcl-2-p53 Axis. Arch Med Res 2020;51(3):233–244; doi: 10.1016/j.arcmed.2020.02.005.

29. Kale J, Osterlund EJ, Andrews DW. BCL-2 family proteins: changing partners in the dance towards death. Cell Death Differ 2018;25(1):65–80; doi: 10.1038/cdd.2017.186.

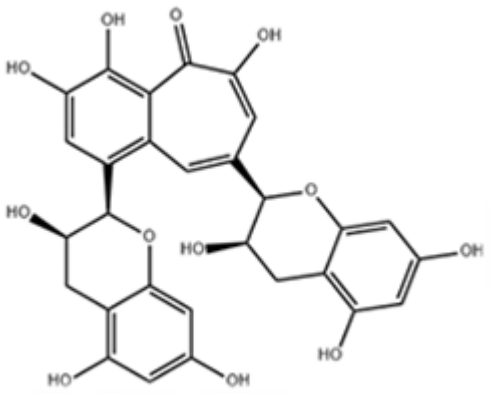

Figure 1. Chemical structure of theaflavin-1 (TF1).

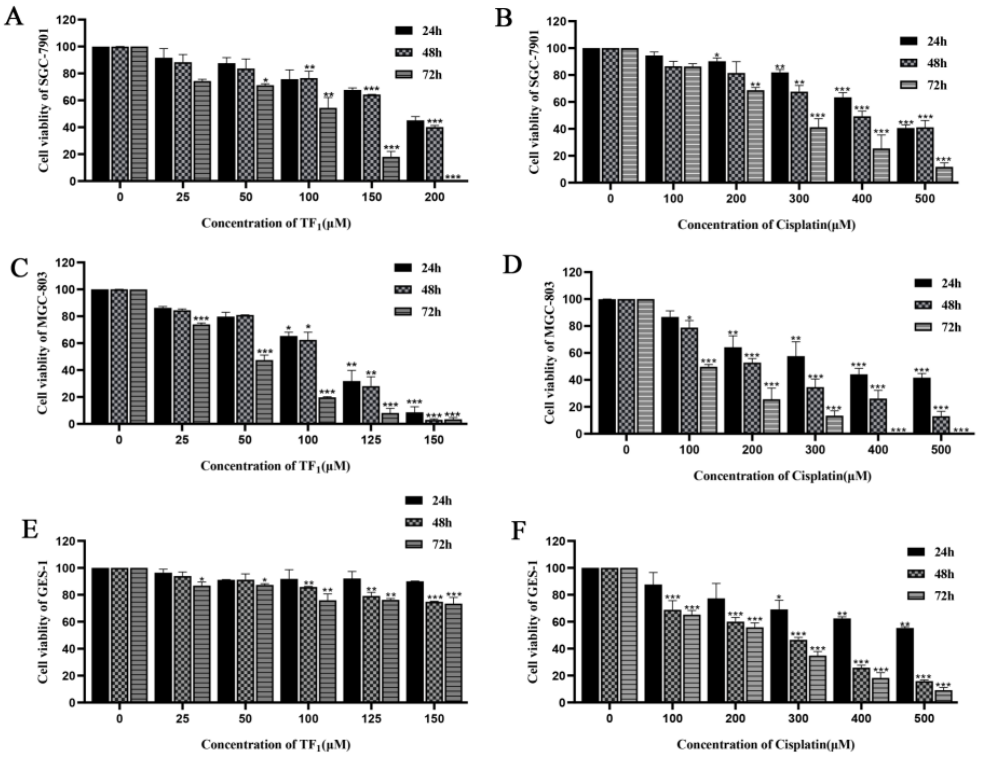

Figure 2 Effects of TF1 and cisplatin on the viability of gastric cancer cells and normal gastric epithelial cells.

Cell viability was determined by CCK-8 assay after treatment with different concentrations of TF1 or cisplatin for 24, 48, and 72 h. (A, C, E) Effect of TF1 on the viability of SGC-7901 cells, MGC-803 cells and GES-1 cells. (B, D, F) Effect of cisplatin on the viability of SGC-7901 cells, MGC-803 cells and GES-1 cells. Data are presented as mean ± SD of three independent experiments. *P < 0.05, **P < 0.01, ***P < 0.001 versus the control group.

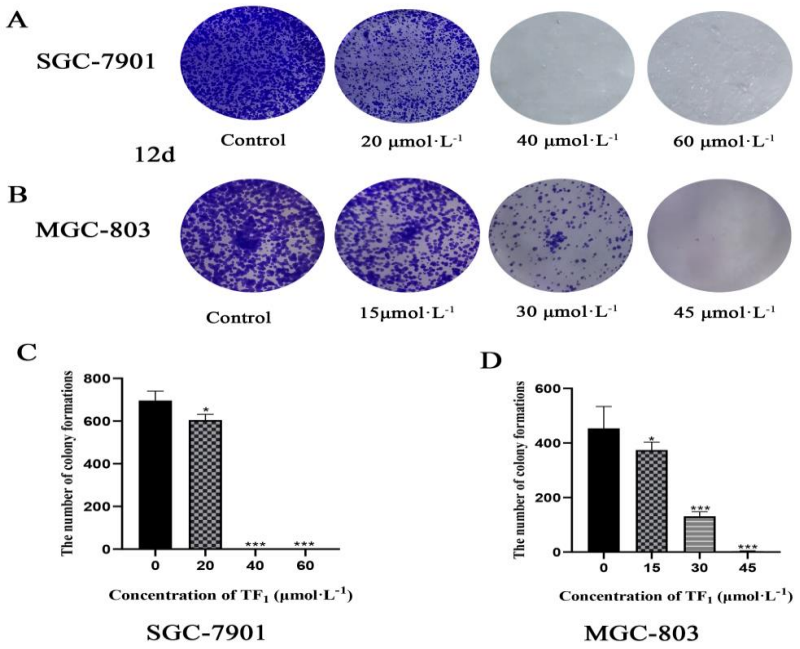

Figure 3 TF1 inhibits colony formation in gastric cancer cells.

Colony formation assays were performed to evaluate the long-term proliferative capacity of gastric cancer cells after TF1 treatment for 12 days.(A, B) Representative images of colony formation in SGC-7901 cells and MGC-803 cells. (C, D) Quantitative analysis of colony numbers in SGC-7901 cells and MGC-803 cells. Data are presented as mean ± SD of three independent experiments. *P < 0.05, ***P < 0.001 versus the control group.

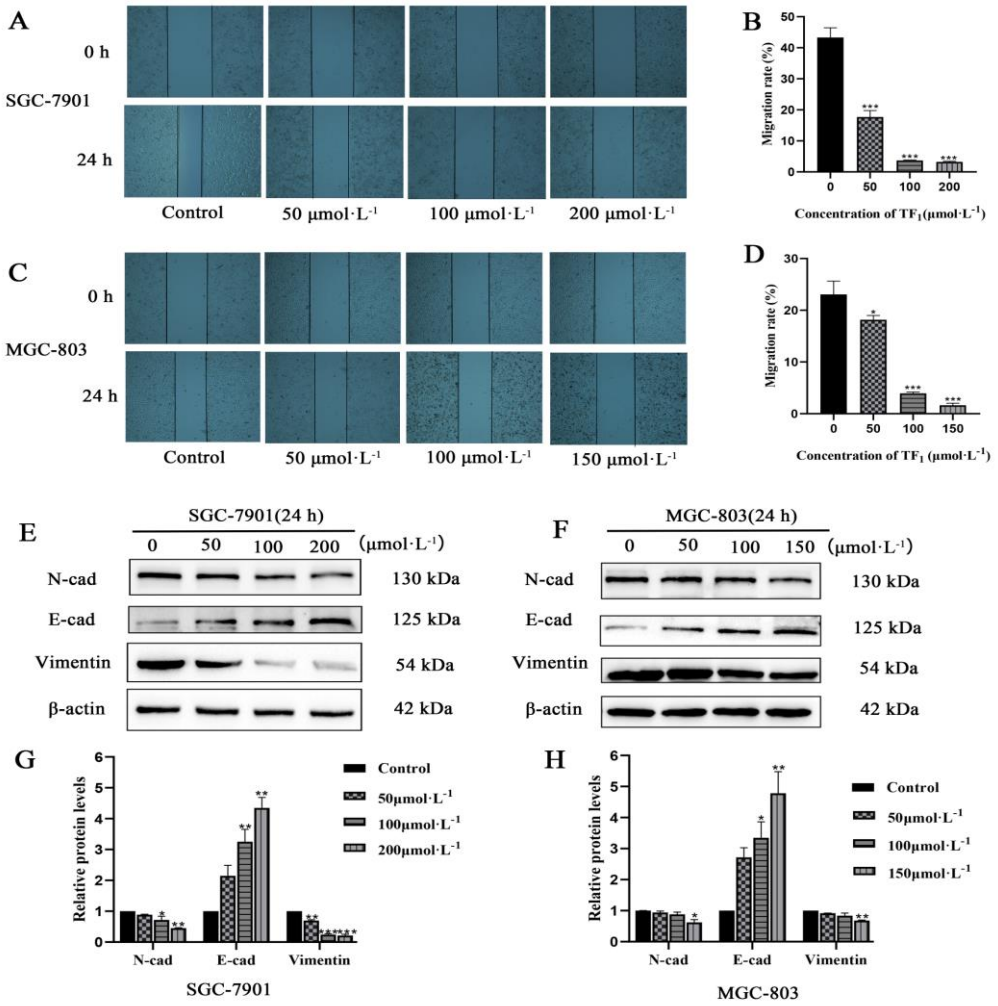

Figure 4 TF1 inhibits migration and EMT in gastric cancer cells.

The effects of TF1 on cell migration were assessed by wound-healing assay, and the expression of EMT-related proteins was determined by western blotting after treatment. (A, C) Representative wound-healing images of SGC-7901 cells and MGC-803 cells. (B, D) Quantitative analysis of the migration rate of SGC-7901 cells and MGC-803 cells. (E, F) Western blot analysis of N-cadherin, E-cadherin, and Vimentin expression in SGC-7901 cells and MGC-803 cells. (G, H) Quantitative analysis of EMT-related protein expression in SGC-7901 cells and MGC-803 cells. Data are expressed as mean ± SD of three independent experiments. *P < 0.05, **P < 0.01, ***P < 0.001 versus the control group.

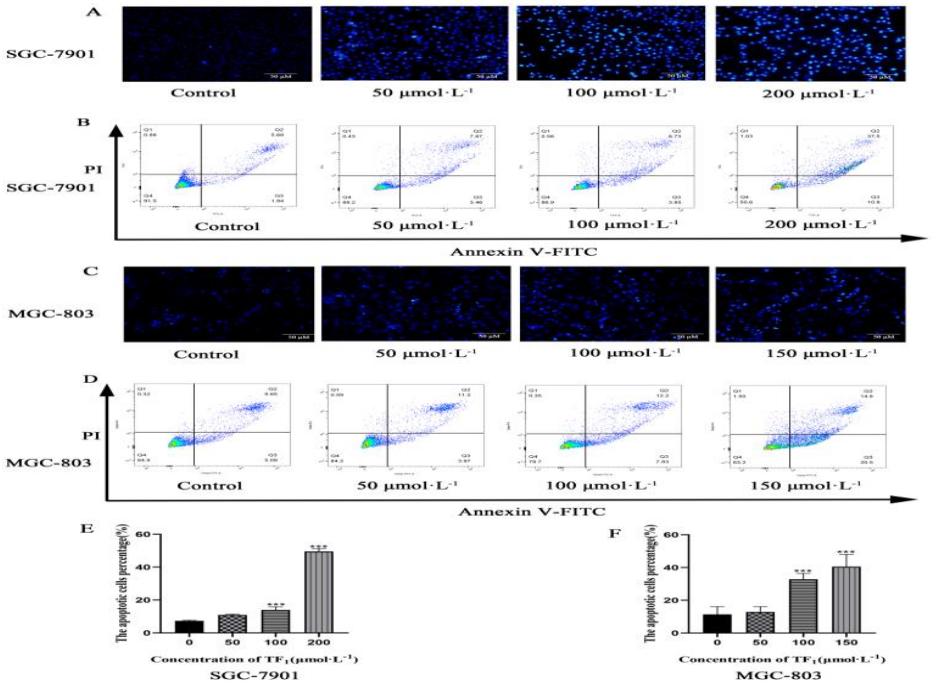

Figure 5 TF1 induces apoptosis in gastric cancer cells.

Apoptosis was evaluated by Hoechst 33258 staining and Annexin V-FITC/PI flow cytometry after TF1 treatment. (A, C) Representative Hoechst 33258 staining images of SGC-7901 cells and MGC-803 cells. (B, D) Representative flow cytometric analysis of apoptosis in SGC-7901 cells and MGC-803 cells. (E, F) Quantitative analysis of apoptotic cell percentages in SGC-7901 cells and MGC-803 cells. Data are presented as mean ± SD of three independent experiments. ***P < 0.001 versus the control group.

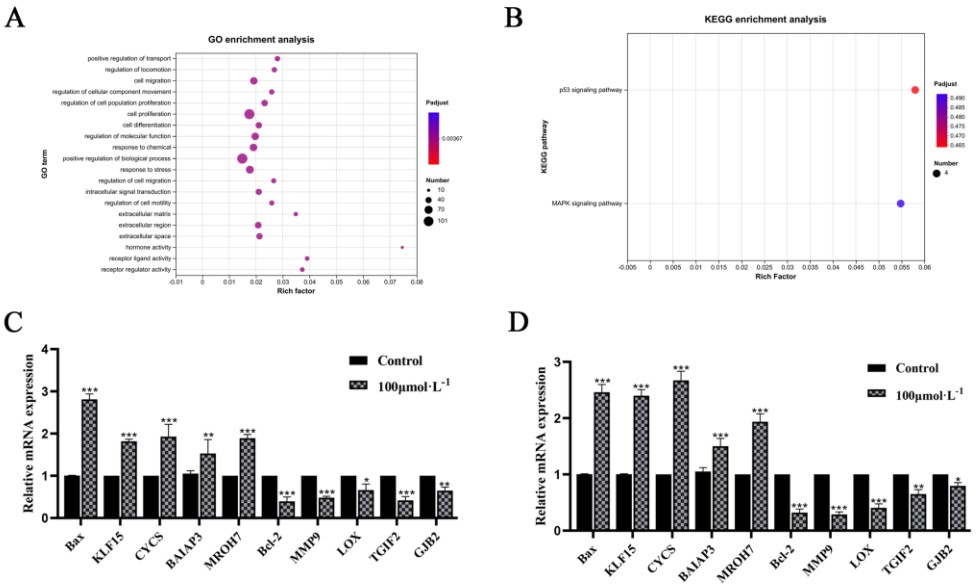

Figure 6 TF1 regulates the p53 signaling pathway in gastric cancer cells.

Transcriptome sequencing and qRT-PCR validation were performed to investigate the molecular mechanisms of TF1 in gastric cancer cells. (A) Gene Ontology enrichment analysis of differentially expressed genes after TF1 treatment. (B) KEGG pathway enrichment analysis showing the major signaling pathways affected by TF1 treatment. (C, D) qRT-PCR validation of selected differentially expressed genes in SGC-7901 cells and MGC-803 cells. Data are expressed as mean ± SD of three independent experiments. *P < 0.05, **P < 0.01, ***P < 0.001 versus the control group.

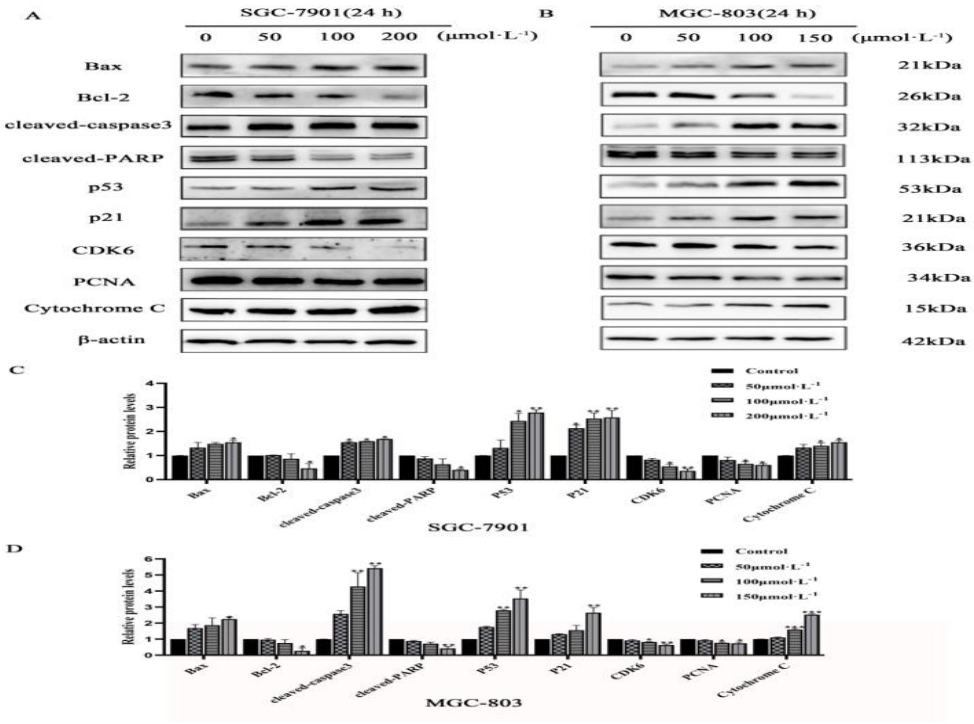

Figure 7 TF1 regulates apoptosis-related proteins in gastric cancer cells.

Western blotting was performed to assess the effects of TF1 on proteins involved in p53 signaling, cell proliferation, and mitochondrial apoptosis after treatment. (A, B) Western blot analysis of Bax, Bcl-2, cleaved-caspase-3, cleaved-PARP, p53, p21, CDK6, PCNA, cytochrome c, and β-actin in SGC-7901 cells and MGC-803 cells. (C, D) Quantitative analysis of protein expression in SGC-7901 cells and MGC-803 cells. Data are presented as mean ± SD of three independent experiments. *P < 0.05, **P < 0.01, ***P < 0.001 versus the control group.

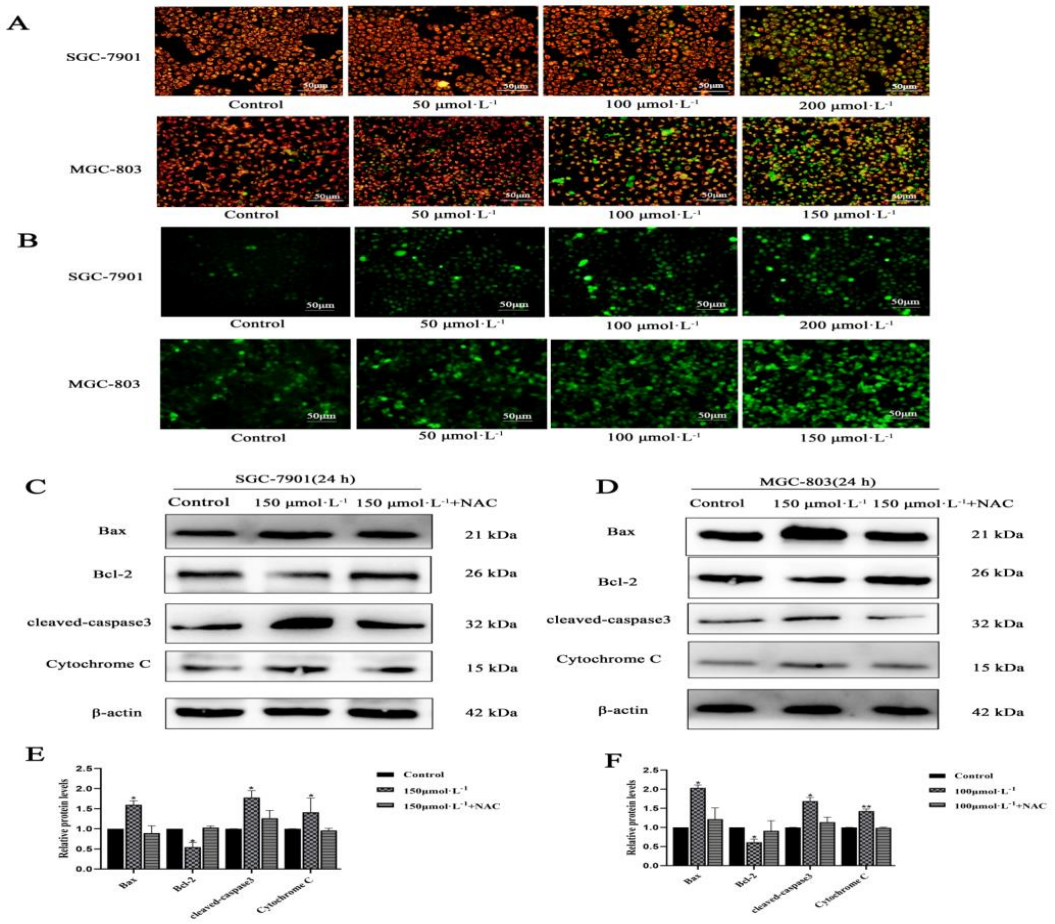

Figure 8. TF1 induces mitochondrial dysfunction and ROS generation.

Mitochondrial membrane potential was evaluated by JC-1 staining, intracellular ROS generation was detected by fluorescence staining, and apoptosis-related proteins were analyzed by western blotting after TF1 treatment with or without NAC pretreatment. (A) Representative JC-1 staining images showing changes in mitochondrial membrane potential in SGC-7901 and MGC-803 cells. (B) Representative fluorescence images showing intracellular ROS levels in SGC-7901 and MGC-803 cells. (C, D) Western blot analysis of Bax, Bcl-2, cleaved-caspase-3, cytochrome c, and β-actin in SGC-7901 cells and MGC-803 cells treated with TF1 alone or TF1 plus NAC. (E) Quantitative analysis of protein expression in SGC-7901 cells and MGC-803 cells. Data are expressed as mean ± SD of three independent experiments. *P < 0.05, **P < 0.01 versus the control group.

Table 1. Primer sequences used for qPCR analysis.

Gene Name	Primer Sequences		Amplification Length
Bax	Forward primer	5′- TTTTGCTTCAGGGTTTCATC-3′	147bp
	Reverse primer	5′-TGTTACTGTCCAGTTCGTCC-3′	
CYCS	Forward primer	5′-AGTCTGCCCTTTCTTCCTTC-3′	146 bp
	Reverse primer	5′-ATACTCTTACACAGCCGCCA-3′	
KLF15	Forward primer	5′-CTCTGAAGATGACAGCGATG-3′	126 bp
	Reverse primer	5′-AATAGGAAGTCCAAGATGCT-3′	
BAIAP3	Forward primer	5′-GGCCCCTGAGGATTTCACGA-3′	141 bp
	Reverse primer	5′-CATGGCGGGTGACCTCCTT-3′	
MROH7	Forward primer	5′-AGCACAAGTTCAAAGGAAAC-3′	100 bp
	Reverse primer	5′-CAATCAGGGTCACATACGAG-3′	
Bc1-2	Forward primer	5′-TGTGTGTGGAGAGCGTCAAC-3′	178 bp
	Reverse primer	5′-CACAGCCAGGAGAAATCAAA-3′	
MMP9	Forward primer	5′-CCAAAACTACTCGGAAGACT-3′	144 bp
	Reverse primer	5′-GCGACACCAAACTGGATGAC-3′	
GJB2	Forward primer	5′-CCACCAGCATTGGAAAG-3′	168 bp
	Reverse primer	5′-CGGAGATGCCGAAGTAGT-3′	
LOX	Forward primer	5′-GCGGAGGAAAACTGTCTGGC-3′	134 bp
	Reverse primer	5′-TATCTTGGTCGGCTGGGTAA-3′	
TGIF2	Forward primer	5′-GCACCGCTACAACGCCTACC-3′	146 bp
	Reverse primer	5′-GGTCTTTGCCATCCTTCCGA-3′	
β-actin	Forward primer	5′-CATGTACGTTGCTATCCAGGC-3′	250 bp
	Reverse primer	5′-CTCCTTAATGTCACGCACGAT-3′	

Table 2. The IC50 values of TF_1 respectively on SGC-7901 and MGC-803 cells for 24, 48, and 72h

Time	IC_{50}(μM)		
	SGC-7901	MGC-803	GES-1
24h	148.24±11.83	99.43±5.37	>500
48h	142.43±8.33	94.22±4.78	
72h	80.52±4.67	59.77±0.24	

Table 3. The IC50 values of cisplatin respectively on SGC-7901、MGC-803 and GES-1 cells for 24, 48, and 72h

Time	IC_{50}(μM)		
	SGC-7901	MGC-803	GES-1
24h	461.67±14.32	379.74±40.81	495.494±13.24
48h	418.52±33.94	259.62±9.26	271.54±11.93
72h	287.76±23.43	141.11±9.02	234.01±2.08